

Finite Conductivity Uniform GTD Versus Knife Edge Diffraction in Prediction of Propagation Path Loss

RAYMOND J. LUEBBERS, MEMBER, IEEE

Abstract—Diffraction propagation over hills and ridges at VHF and UHF is commonly estimated using Fresnel knife edge diffraction. This approach has the advantage of simplicity, and for many geometries yields accurate results. However, since it neglects the shape and composition of the diffracting surface, it can in some cases yield results which are in serious disagreement with measurements. To remedy this, attempts have been made to approximate the diffracting hill or ridge by other shapes, most notably cylinders. These approaches have not been widely adopted, due in large part to their greater numerical complexity. In this paper it is proposed to apply wedge diffraction in the format of the geometrical theory of diffraction (GTD), modified to include finite conductivity and local surface roughness effects. It is shown that, for geometries with grazing incidence and/or diffraction angles, significant improvement in accuracy is obtained. Further, the GTD wedge diffraction form used is based on the Fresnel integral, so that it is only slightly more complex numerically than knife edge diffraction. Finally, the GTD includes reflections from the sides of the ridge (wedge faces), and can be extended to multiple ridge diffraction and three-dimensional terrain variations.

I. INTRODUCTION

PREDICTION OF effects of intervening terrain on the propagation of high frequency electromagnetic waves has important applications in the siting and evaluation of ground-to-ground and ground-air communication links and in assessing the performance of low altitude radar. The problem is a complex one, and any practical solution requires simplifying assumptions. For the present discussion the frequency range will be limited from 100 MHz to 10 GHz, so that the dominant propagation mechanism is the space wave, and the surface wave will be neglected. It will be assumed that the terrain between the transmitting and receiving antennas is described with sufficient accuracy such that a deterministic rather than probabilistic estimate of the path loss is feasible. Finally, it will be assumed that the terrain variation transverse to the propagation path has negligible effect on the path loss.

For intervening terrain which has one dominant diffracting ridge, the method of Fresnel knife edge diffraction, proposed in the classic paper by Schelleng, Burrows, and Ferrell [1], is still in wide use. Their approach applied knife edge diffraction, extended using image theory to include reflections from any relatively level ground which might exist between the ridge and the transmission or reception points. If such reflections can be neglected, then the simple single-ray knife edge diffraction result can be expressed graphically, as by Bullington [2], whose method is currently in general use.

For many cases in the literature, reasonably good results using knife edge diffraction have been reported [3], [4], [5]. However, in other cases poor agreement with measurements has been obtained [6]. This is not surprising, since the knife edge approximation ignores such important parameters as polarization, conductivity and permittivity, ridge profile, and surface roughness.

Several attempts have been made to include the effects of the profile of the diffracting ridge by modeling it as a circular or parabolic cylinder [7]–[10]. These solutions have, in some cases, been applied by their authors or others with good results. However, they have not received wide application. The cylindrical diffraction solutions are significantly more complex numerically than knife edge diffraction, are not applicable in many cases due to limitations placed on the radius of curvature of the ridge, and show large variation between vertical and horizontal polarization which is contrary to observation. And, as with knife edge diffraction, reflection from the hillside forming the diffracting ridge cannot be readily included.

Another approach is to approximate the diffracting ridge as a wedge. Wedge diffraction solutions have been available since the beginning of the century, but have not been widely used for propagation path loss predictions due to complexity. A numerically simple and elegant solution to wedge diffraction which serves as a canonical problem in the geometrical theory of diffraction (GTD) was published by Keller 20 years ago [11]. However, it was not suitable for general application to radio propagation over diffracting edges since it fails in the vicinity of shadow boundaries, i.e., when the source, edge, and field point lie on a straight line. This shortcoming was eliminated by Kouyoumjian and Pathak [12] in their formulation of a wedge diffraction coefficient which is valid at shadow and reflection boundaries. Furthermore, their formulation is only slightly more involved numerically than simple knife edge diffraction, as it is also based upon the Fresnel integral. The geometrical theory of diffraction is an extension of geometrical optics, so that the effects of rays reflected from the side of the diffracting ridge, and their interference with direct and diffracted rays, can be included.

As originally formulated, the diffraction coefficients were limited to perfectly conducting wedges. Recently, a heuristic extension which allows the approximate treatment of finitely conducting locally rough wedge diffraction has been made [13], [14]. It is this form of wedge diffraction which will be considered here, limited to two-dimensional terrain.

In addition to the already mentioned advantages of including finite conductivity and local surface roughness effects, the diffracting edge profile, and reflection from the wedge faces, the GTD is capable of other extensions. Multiple diffraction from successive ridges can be included, with certain limitations [15], [16]. This can be combined with intermediate reflections to produce a general reflection-diffraction model [14] capable of predicting propagation path loss over arbitrary two-dimensional terrain. The GTD is three-dimensional, so at the expense of computational complexity it can also be used to predict path loss effects of three-dimensional terrain irregularities.

Despite other alternatives, the most widely used technique for making deterministic predictions of diffraction loss is knife edge diffraction. The purpose of this paper is to show that, with a minor increase in computation effort, wedge diffraction can be

Manuscript received January 14, 1983; revised August 26, 1983.

The author is with the Advanced Electronics Laboratory, Lockheed Palo Alto Research Laboratory, 3251 Hanover Street, Palo Alto, CA 94304.

on in

used to obtain path loss predictions that will agree with knife edge diffraction for the cases where it is valid, and be significantly more accurate where it is not.

II. FORMULATION

Referring to Fig. 1, consider a field point in the shadow region, such that geometrical optics predicts zero electric field. The source radiates an arbitrarily polarized spherical wave. If we denote by E_0 the relative source amplitude, then knife edge diffraction would predict the electric field at the field point as

$$E_{KE} = E_0 \frac{e^{-jk(d_1+d_2)}}{d_1+d_2} \cdot \frac{1+j}{2} \cdot \int_v^\infty e^{-j(\pi/2)\tau^2} d\tau \quad (1)$$

where

$$v = u \sqrt{\frac{2(d_1+d_2)}{\lambda d_1 d_2}} \quad (2)$$

under the conditions that $d_1, d_2 \gg u$ and $d_1, d_2 \gg \lambda$.

The GTD formulation for the electric field at the field point is given by [12], specializing to two dimensions,

$$E_{GTD} = E_0 \frac{e^{-jks'}}{s'} D_{\parallel}^{\pm} \sqrt{\frac{s'}{s(s'+s)}} e^{-jks} \quad (3)$$

where D_{\parallel}^{\pm} represents the diffraction coefficient, which will depend upon the polarization (perpendicular or parallel to the plane of incidence) of the incident field on the edge. If the field point is not close to a shadow or reflection boundary, and the wedge is perfectly conducting, then the diffraction coefficient is given by [11] as

$$D_{\parallel}^{\pm} = \frac{e^{-j\pi/4 \sin(\pi/n)}}{n\sqrt{2\pi k}} \left[\frac{1}{\cos(\pi/n) - \cos\left(\frac{\phi - \phi'}{n}\right)} \mp \frac{1}{\cos(\pi/n) - \cos\left(\frac{\phi + \phi'}{n}\right)} \right] \quad (4)$$

where ϕ' and ϕ are the angles of incidence and diffraction and π is the exterior wedge angle. However, if it is desired to evaluate the field diffracted by a finitely conducting, locally rough wedge, then the results of [12], [13], and [14] can be combined to give

$$D_{\parallel}^{\pm} = \frac{e^{-j\pi/4}}{2n\sqrt{2\pi k}} \times \left\{ \cot\left(\frac{\pi + (\phi - \phi')}{2n}\right) \cdot F(kLa^{\pm}(\phi - \phi')) \mp \cot\left(\frac{\pi - (\phi - \phi')}{2n}\right) \cdot F(kLa^{\mp}(\phi - \phi')) \right. \\ \left. \mp R_0^{\pm} \cdot \cot\left(\frac{\pi - (\phi + \phi')}{2n}\right) \cdot F(kLa^{\mp}(\phi + \phi')) \mp R_n^{\pm} \cdot \cot\left(\frac{\pi + (\phi + \phi')}{2n}\right) \cdot F(kLa^{\pm}(\phi + \phi')) \right\} \quad (5)$$

where

$$F(x) = 2j\sqrt{x} e^{ix} \int_{\sqrt{x}}^{\infty} e^{-j\tau^2} d\tau \quad (6)$$

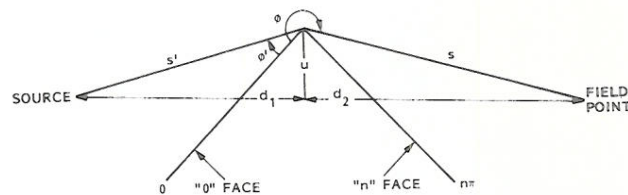


Fig. 1. Geometry and coordinates for application of both wedge and knife edge diffraction.

and is also a Fresnel integral,

$$L = \frac{ss'}{s+s'} \quad (7)$$

$$a^{\pm}(\beta) = 2 \cos^2\left(\frac{2n\pi N^{\pm} - \beta}{2}\right), \quad \beta = \phi \pm \phi' \quad (8)$$

In (8), N^{\pm} are the integers which most nearly satisfy the equations

$$2n\pi N^+ - \beta = \pi \quad (9a)$$

$$2n\pi N^- - \beta = -\pi \quad (9b)$$

R_0^{\perp}, R_n^{\perp} are the reflection coefficients for either perpendicular or parallel polarization for the 0 face, incidence angle ϕ' , and for the n face, reflection angle $n\pi - \phi$. For the computations included in this paper, the usual finite conductivity dielectric plane wave reflection coefficients (for example, [17]), modified for surface roughness ([14], [18]), are used. If $R_0^{\parallel}, R_n^{\parallel}$ are replaced by ∓ 1 , the perfect conductivity formulation of [12] is obtained.

At shadow and reflection boundaries one of the cotangent functions becomes singular. However, D_{\parallel}^{\pm} remains finite, and can be readily evaluated. The term containing the singular cotangent function is given for small ϵ by [12] as

$$\cot\left(\frac{\pi \pm \beta}{2n}\right) F(kLa^{\pm}(\beta)) \cong n[\sqrt{2\pi kL} \operatorname{sgn} \epsilon - 2kLe^{j\pi/4}] \cdot e^{j\pi/4} \quad (10)$$

with ϵ defined by

$$\beta = 2n\pi N^{\pm} \mp (\pi - \epsilon) \quad (11)$$

The resulting diffraction coefficient will be continuous at shadow and reflection boundaries, provided that the same reflection coefficient is used when calculating reflected rays. The finite conductivity-surface roughness modification is approximate; however, reported results agree well with measurements [13], [14], [19].

While the above expressions for the diffraction coefficient may appear complicated compared with knife edge diffraction, a computer subroutine for their evaluation may be written quite readily, or obtained by modification of perfect conductivity diffraction coefficient subroutines available in the literature [20].

Referring to Fig. 1, if $n \approx 2$, knife edge and GTD results are nearly identical. However, in many actual propagation applications, $n \approx 1$, ϕ' is small, and ϕ is nearly equal to $n\pi$, so that significant differences exist. The following sections will point out some of these differences.

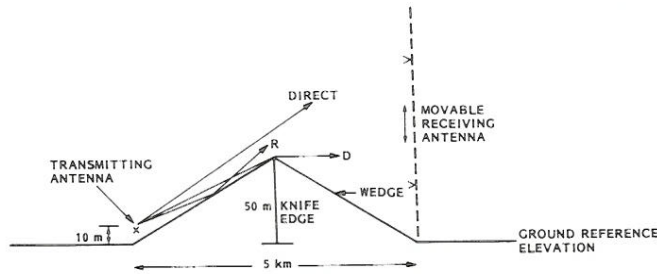


Fig. 2. Idealized terrain profile used to illustrate differences between GTD wedge diffraction and knife edge diffraction. The rays included in the GTD calculations (direct, reflected (R), diffracted (D)) are illustrated.

III. BASIC DIFFERENCES BETWEEN KNIFE EDGE AND WEDGE DIFFRACTION

While the two approaches yield almost identical answers for the cases where knife edge diffraction is valid, the philosophy of the two methods is very different. Knife edge diffraction is applied by considering secondary Huygen's sources in the plane of the knife edge, with the "knife" considered as an ideal absorber. Thus one integrates over the unobstructed half-plane above the knife edge to find the total field transmitted over the edge.

The GTD, on the other hand, is an extension of geometrical optics. Energy may travel from the source to the field point by a direct path, by reflection, by diffraction, or by combinations of these processes. Direct, reflected, and diffracted rays, unless shadowed by intervening terrain, are added to give the total transmitted field. This capability of including different transmission mechanisms makes the GTD a much more powerful method.

Consider the idealized two-dimensional terrain profile of Fig. 2. A 5 km path containing a single ridge 50 m high separates the transmitting and receiving antennas. It is desired to determine the propagation path loss between the two antennas as a function of receiving antenna height. The knife edge solution assumes a vertical knife edge at the apex of the ridge; the GTD considers the entire ridge as a wedge. For this geometry the interior wedge angle is 178° . For receiving antenna heights below 90 m (the shadow boundary), only the diffracted ray, calculated as described previously, is included in the GTD solution; above 90 m, the direct ray is added; above 110 m (the reflection boundary), the singly reflected ray is also added, emanating from the image of the transmitting antenna in the ridge upslope.

Fig. 3 shows the results obtained using knife edge diffraction, Fig. 4 with perfect conductivity GTD ($R_{0,n} = \mp 1$), and Fig. 5, GTD with finite conductivity and local surface roughness. The differences are quite striking. Comparing first Figs. 3 and 4, the perfect conductivity GTD results show a considerable difference with polarization, while the knife edge results do not. This difference is due, of course, to the fact that the reflection coefficient for parallel polarized electric field is $+1$ for a perfectly conducting plane, but nearly -1 for finitely conducting and grazing incidence. So in this regard the knife edge results are more in agreement with measurements of propagation loss over actual terrain, which typically show little effect of polarization. In the shadowed region, the perfect conductivity GTD result shows considerably more attenuation than knife edge diffraction for perpendicular polarization, considerably less for parallel. In the

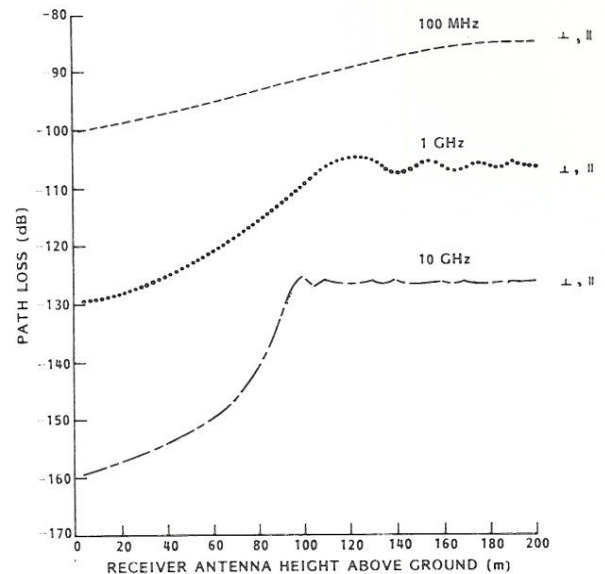


Fig. 3. Path loss in dB versus antenna height for the idealized terrain profile of Fig. 2 calculated using knife edge diffraction at 0.1, 1.0, and 10.0 GHz, for both polarizations.

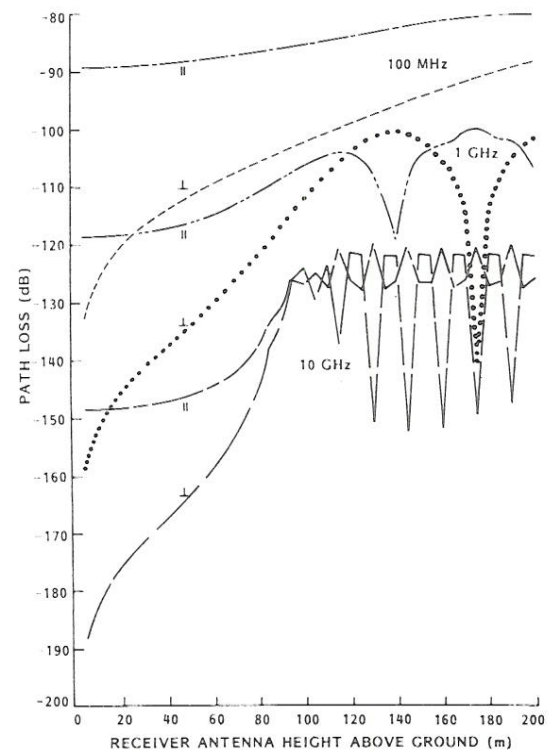


Fig. 4. Path loss in dB versus antenna height for the idealized terrain profile of Fig. 2 calculated for both polarizations using the GTD, including direct, reflected, and diffracted rays, and assuming smooth perfectly conducting surfaces.

interference region above the reflection boundary, the perfect conductivity GTD result shows the expected interference pattern at the higher frequencies, while the knife edge solution cannot include this effect. However, the null depths predicted by the perfect conductivity GTD results, especially at the highest frequency, are much deeper than would be produced by actual terrain.

Considering the finite conductivity GTD results of Fig. 5, there are two important improvements over the results of Fig. 4. First

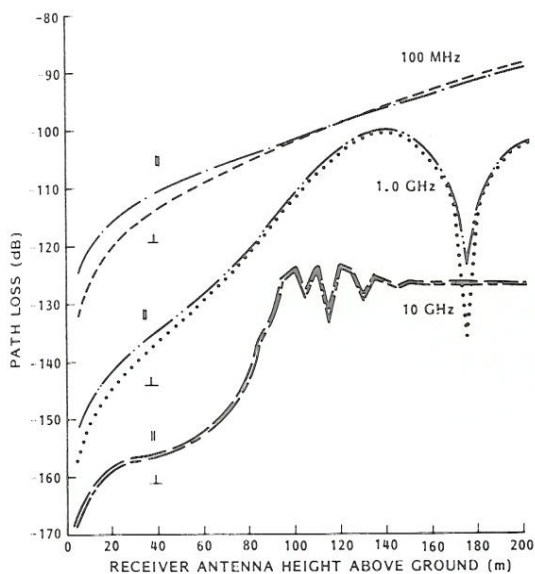


Fig. 5. Path loss in dB versus antenna height for the idealized terrain profile of Fig. 2 calculated for both polarizations using the GTD, including direct, reflected, and diffracted rays, and assuming terrain parameters $\sigma = 0.012$ s/m, $\epsilon_r = 15.0$, and standard deviation of surface roughness = 0.5 m.

parallel and perpendicular polarization show much less difference, especially at higher frequencies, which is in agreement with the majority of measured data. One could produce exactly the same result for both polarizations by using $R = -1$ for both, arguing that at grazing incidence the reflection coefficient for both polarizations is approximated by that value. However, the finite conductivity GTD is capable of including reflections from finitely conducting wedge faces for incidence angles where the reflection coefficient is not well approximated by -1 , for example at high frequencies where local surface roughness reduces the amplitude of the reflected signal, or for vertical polarization for ground-to-air or air-to-air communications where the incidence angles can be well above grazing. This capability is the reason for the second significant improvement over the perfectly conducting results of Fig. 4, the realistic null depths in the interference region above the reflection boundary which are evident in the 10 GHz curves of Fig. 5. This is due to the reduction in amplitude of the reflections from the wedge face due to the assumed local surface roughness standard deviation of 0.5 m.

Comparing Figs. 3 and 5, the GTD solution predicts significantly more attenuation than knife edge diffraction as the field point approaches the wedge face, as would be expected due to the reflection coefficient being approximately -1 , indicating almost zero electric field at the wedge surface. Above the reflection boundary, the finite conductivity GTD solution result is an interference pattern which averages to the knife edge results.

While the above results agree qualitatively with intuitive expectations of the differences between the solution methods, conclusions regarding the applicability of the various solutions to actual propagation predictions can best be reached by comparison with measured results. This is the purpose of the next section.

IV. APPLICATION TO ACTUAL TERRAIN

While there have been no previous published comparisons of GTD and knife edge predictions of propagation path loss, pre-

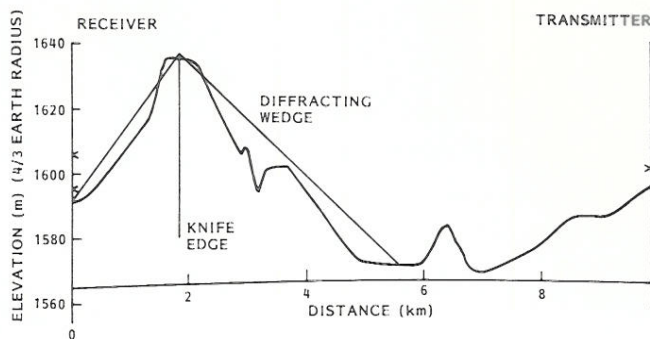


Fig. 6. Actual terrain profile [22, path R1-10-T2A] with total path length 9.82 km, showing wedge and knife edge approximations to dominant diffracting ridge and antenna locations.

vious papers have compared GTD results with physical optics, the Longley-Rice point-to-point model, and measurements [14], [21]. In those papers the GTD model included higher order ray types (e.g., diffracted-reflected-diffracted rays), which cannot be readily duplicated in effect by knife edge diffraction. The accuracy of the GTD formulation in dealing with terrain profiles where reflection is the dominant interaction mechanism, and where the field point moves through shadow and reflection boundaries, has been shown previously [21]. In order to provide a clear display of the fundamental differences between GTD and knife edge diffraction, for the following results the GTD solution will be limited to singly diffracted and diffracted-reflected rays, and the terrain profiles chosen such that diffraction from a single dominant ridge is the primary propagation means. For all of the profiles and antenna configurations considered in the following, the 14-ray GTD model of [14] was used to predict path loss on a piecewise-linear terrain profile of the entire path, and in all cases was within a few dB of the limited GTD results reported here, which would be expected since the paths were chosen to emphasize diffraction from a single edge. The notable exceptions were that the 14-ray GTD model did predict the fine structure evident in the results of Fig. 13 for low antenna heights, and did not have the discontinuities seen at 20 ft in Figs. 11 and 12, due to the reflection point moving to the adjacent plate.

Let us first consider the terrain profile of Fig. 6, and corresponding path loss measurements of Figs. 7-9, taken from [22]. For the GTD solution the dominant diffracting ridge is approximated by a wedge as shown in Fig. 6. The wedge angle is 177.6° , and the field point is located above the base of the ridge. This situation approximates that of the lower antenna heights of the hypothetical terrain profile of Fig. 2.

Path loss as calculated using knife edge diffraction with the knife edge located at the apex of the wedge, for both finitely and perfectly conducting GTD, and measured values for 230, 1846, and 9190 MHz are shown in Figs. 7-9. As expected from the previous results, the GTD predicted path losses are significantly below knife edge, especially at the lower frequencies, and quite clearly agree much more closely with the measured results, especially for field points closer to the ground. Only horizontally polarized measured results are available. For this situation there is no significant difference between the two GTD predictions, except at the highest frequency (due to surface roughness).

While the previous results point out the significant improvement which can be obtained using GTD, the situation was a rather special one in which the field point was located just at the base of the diffracting ridge. Knife edge diffraction is not typically

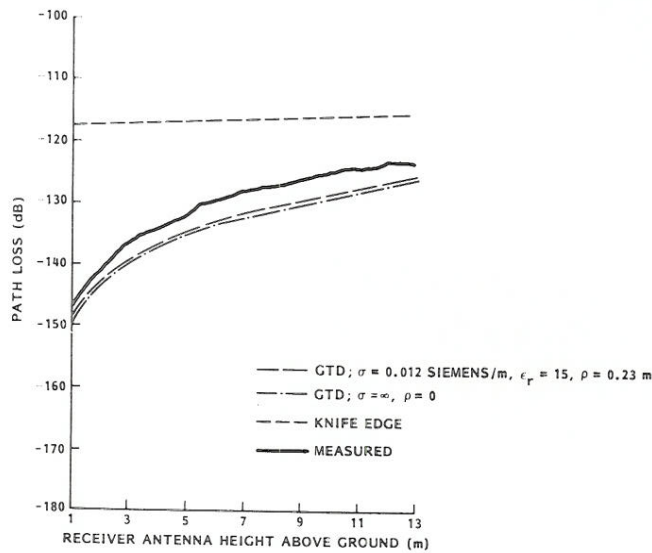


Fig. 7. Calculated and measured path loss versus receiving height above local terrain for the terrain profile of Fig. 6 at 230 MHz. Transmitting antenna height above local terrain is 6.6 m. Only singly diffracted ray included in GTD. Horizontal (1) polarization.

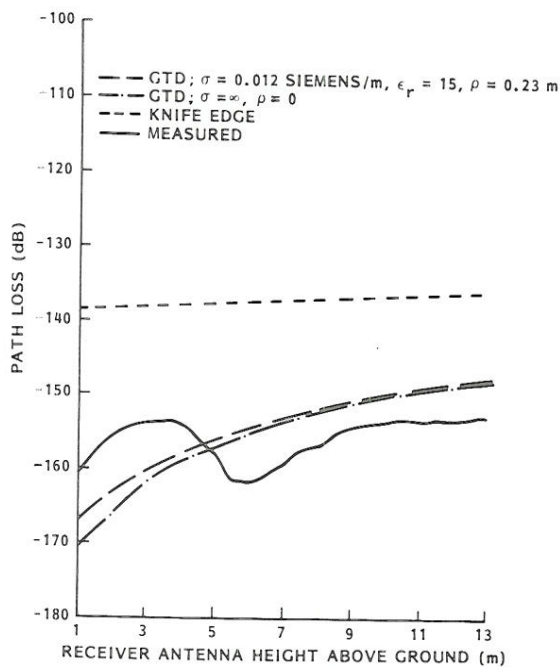


Fig. 8. Calculated and measured path loss versus receiving antenna height above local terrain for the terrain profile of Fig. 6 at 1846 MHz. Transmitting antenna height above local terrain is 7.3 m. Only singly diffracted ray included in GTD. Horizontal (1) polarization.

applied to such a situation, but rather when the source and field points are distant from the dominant diffracting ridge. For situations where the wedge angle of the ridge is relatively small, and the incident and diffracted rays are sufficiently removed from grazing, wedge and knife edge diffraction will give essentially identical results, and good agreement with measured results can be obtained by both. However, in many situations the above conditions are not met, and an example of such is shown in the terrain profile of Fig. 10, which is taken, along with the subsequent path loss measurements, from [6]. The elevations have been adjusted for earth curvature using $4/3$ earth radius. The linearized diffracting wedge has an angle of 177.0° , with mini-

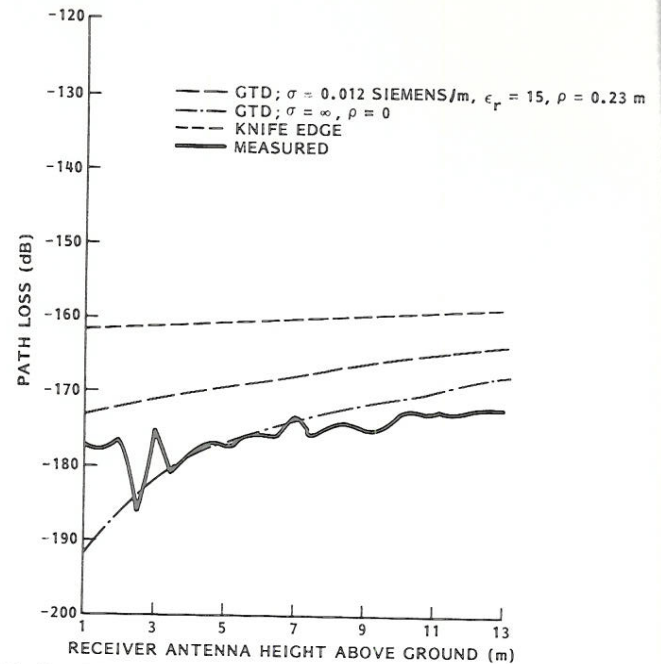


Fig. 9. Calculated and measured path loss versus receiving antenna height above local terrain for the terrain profile of Fig. 6 at 9190 MHz. Transmitting antenna height above local terrain is 7.3 m. Only singly diffracted ray included in GTD. Horizontal (1) polarization.

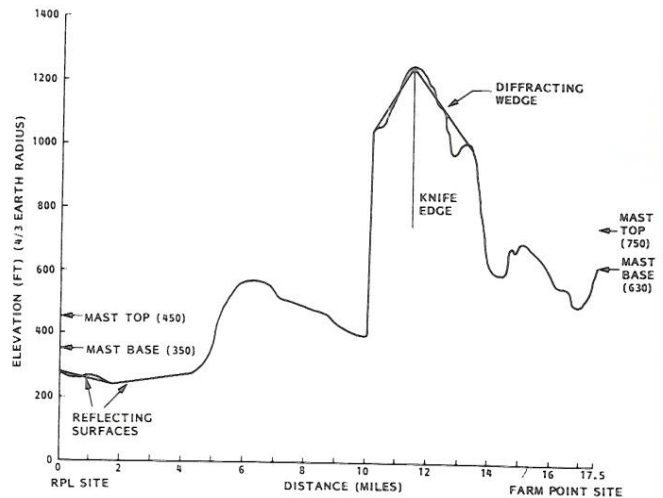


Fig. 10. Actual terrain profile [6] with total path length 17.5 mi (28.2 km), showing wedge and knife edge approximations to dominant diffracting ridge. Both methods include reflections from indicated surfaces at RPL end of path when possible.

imum incidence angles of the ray with the wedge faces of 0.821° and 0.303° . Reflections from the (linearized) terrain just in front of the Radio Physics Laboratory (RPL) site were included in both the GTD and knife edge results.

Figs. 11 and 12 contain calculated and measured results for 493 MHz with the antenna at the RPL site varied in height, and with the farm point site antenna fixed. For both polarizations the finite conductivity GTD results show very significant improvement in agreement with the measurements over the knife edge results, and for the vertically polarized case over perfect conductivity GTD as well. (To facilitate comparison of the diffraction effects, all reflections have been calculated using finite conductivity and local surface roughness.) The additional measured increase in path loss over the finite conductivity GTD

$\epsilon_r = 15, \rho = 0.23 \text{ m}$

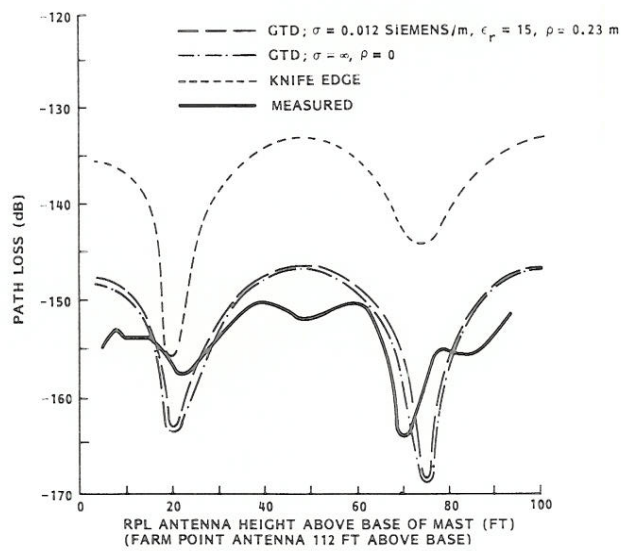


Fig. 11. Calculated and measured path loss versus antenna height for the terrain profile of Fig. 10 at 493 MHz. Horizontal (I) polarization.

13 m)
ing antenna height
9190 MHz. Trans-
i. Only singly dif-
ion.

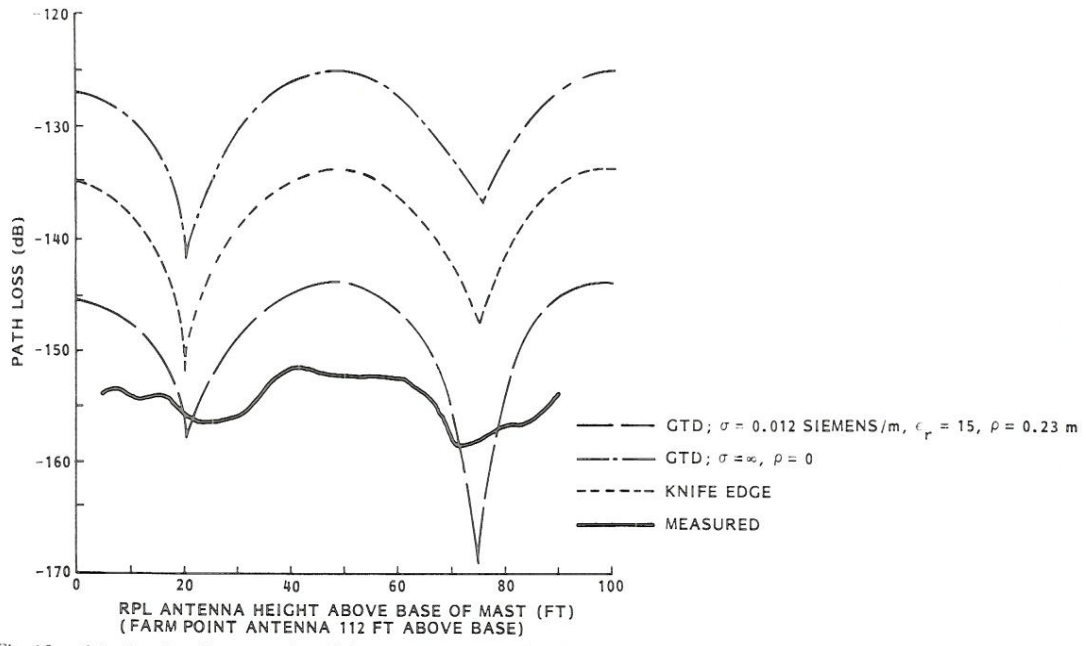
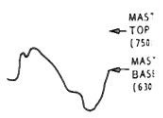


Fig. 12. Calculated and measured path loss versus antenna height for the terrain profile of Fig. 10 at 493 MHz. Vertical (II) polarization.

DIFFR
WEDGE



16 17.5
FARM POINT SITE

length 17.5 mi (28.3
is to dominant dir-
i indicated surface

e faces of 0.821
) terrain just
te were included

measured results for
ed in height, and
both polarizations
y significant in
s the knife
case over perfect
comparison of the
calculated using
) The addition-
conductivity GTD

results is probably due to the effect of the trees which covered the diffracting ridge [6], which would also explain the greater measured loss for vertical polarization, since vertically polarized waves would interact with the vertical tree trunks to a greater extent.

Fig. 13 shows results with the RPL antenna fixed and the farm point antenna height varied. Again finite conductivity GTD results are in significantly better agreement with measurements than knife edge diffraction or perfect conductivity GTD. The finite conductivity GTD reproduces almost exactly the measured rate of decrease in path loss with antenna height, while the knife edge result does not, indicating the validity of modeling the diffracting ridge as a wedge.

V. CONCLUSION

It has been shown that in certain cases significant improvement over knife edge diffraction can be obtained by approximat-

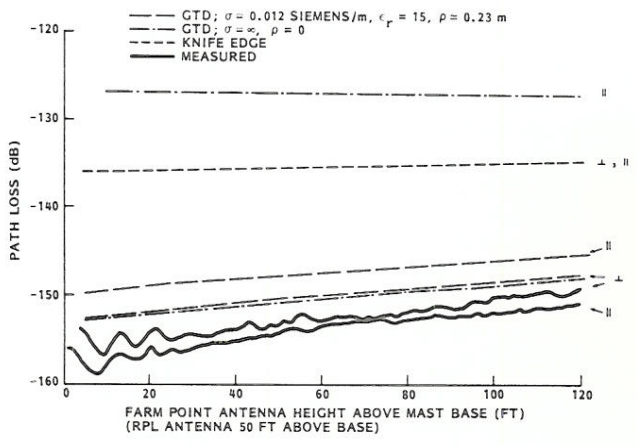


Fig. 13. Calculated and measured path loss versus antenna height for the terrain profile of Fig. 10 at 493 MHz. Both horizontal (I) and vertical (II) polarizations.

ing the diffracting ridge as a finitely conducting, locally rough wedge and applying the geometrical theory of diffraction. This approach furnishes a better approximation to the ridge profile than a knife edge, and can include reflections from the sides of the ridge (wedge faces). The results are most significantly improved with respect to knife edge diffraction for large wedge angles and grazing incidence and/or diffraction angles.

While other attempts have been made to include the ridge cross section more accurately, notably approximating the tip of the ridge as a cylinder, the wedge diffraction approach outlined here has significant advantages. It is numerically more simple, and includes effects of conductivity, local roughness, and reflections from the hillside.

Perhaps most significantly, the approach outlined here using wedge diffraction is applied in the context of the geometrical theory of diffraction, which is a three-dimensional method. Thus extension to three-dimensional terrain, and inclusion of the effects of transverse terrain variations is possible. Other possible extensions include propagation over mixed (conductivity and/or roughness) paths, including effects of trees, and propagation over multiple ridges.

REFERENCES

- [1] J. C. Schelleng, C. R. Burrows, and E. B. Ferrell, "Ultra-short wave propagation," *Bell Syst. Tech. J.*, pp. 125-161, Apr. 1933.
- [2] K. Bullington, "Radio propagation fundamentals," *Bell Syst. Tech. J.*, pp. 593-626, 1957.
- [3] F. H. Dickson *et al.*, "Large reductions of VHF transmission loss and fading by the presence of a mountain obstacle in beyond-line-of-sight paths," *Proc. IRE*, pp. 967-969, Aug. 1953.
- [4] R. S. Kirby *et al.*, "Obstacle gain measurements over Pikes peak at 60 to 1046 Mc," *Proc. IRE*, pp. 1467-1472, Oct. 1955.
- [5] M. L. Meeks, "A propagation experiment combining reflection and diffraction," *IEEE Trans. Antennas Propagat.*, vol. AP-30, pp. 318-321, Mar. 1982.
- [6] J. H. Crysedale *et al.*, "An experimental investigation of the diffraction of electromagnetic waves by a dominating ridge," *IRE Trans. Antennas Propagat.*, pp. 203-210, Apr. 1957.
- [7] H. E. J. Neugebauer and M. P. Bachynski, "Diffraction by smooth cylindrical mountains," *Proc. IRE*, pp. 1619-1627, Sept. 1958.
- [8] J. R. Wait and A. M. Conda, "Diffraction of electromagnetic waves by smooth obstacles for grazing angles," *J. Res. Nat. Bur. Stand.-D. Radio Propagat.*, pp. 181-197, Sept. 1959.
- [9] H. T. Dougherty and L. J. Maloney, "Application of diffractions by convex surfaces to irregular terrain situations," *Radio Sci.*, pp. 239-250, Feb. 1964.
- [10] M. S. de Assis, "A simplified solution to the problem of multiple diffraction over rounded obstacles," *IEEE Trans. Antennas Propagat.*, pp. 292-295, Mar. 1971.
- [11] J. B. Keller, "Geometrical theory of diffraction," *J. Opt. Soc. Amer.*, pp. 116-130, 1962.
- [12] R. G. Kouyoumjian and P. H. Pathak, "A uniform geometrical theory of diffraction for an edge in a perfectly conducting surface," *Proc. IEEE*, pp. 1448-1461, Nov. 1974.
- [13] W. D. Burnside and K. W. Burgener, "High frequency scattering by a thin lossless dielectric slab," *IEEE Trans. Antennas Propagat.*, vol. AP-31, pp. 104-110, Jan. 1983.
- [14] K. C. Chamberlin and R. J. Luebbers, "An evaluation of Longley-Rice and GTD propagation models," *IEEE Trans. Antennas Propagat.*, vol. AP-30, pp. 1093-1098, Nov. 1982.
- [15] R. Tiberio and R. G. Kouyoumjian, "An analysis of diffraction at edges illuminated by transition region fields," *Radio Sci.*, pp. 323-336, Mar.-Apr. 1982.
- [16] Y. Rahmat-Samii and R. Mittra, "On investigation of diffracted fields at the shadow boundaries of staggered parallel plates: A spectral domain approach," *Radio Sci.*, pp. 659-670, 1977.
- [17] E. C. Jordan and K. G. Balmain, *Electromagnetic Waves and Radiating Systems*, 2nd ed. Englewood Cliffs, NJ: Prentice-Hall, 1968, pp. 631-632.
- [18] P. Beckman and A. Spizzichino, *The Scattering of Electromagnetic Waves from Rough Surfaces*. New York: MacMillan, 1963, p. 246.
- [19] R. G. Rojas-Teran and W. D. Burnside, "GTD analysis of airborne antennas in the presence of lossy dielectric layers," Ohio State Univ. Electro-Sci. Lab. Rep. 710964-8, Aug. 1981.
- [20] W. L. Stutzman and G. A. Thiele, *Antenna Theory and Design*. New York: Wiley, 1981, pp. 591-594.
- [21] R. J. Luebbers, V. Ungvichian, and L. Mitchell, "GTD terrain reflection model applied to ILS glide slope," *IEEE Trans. Aerosp. Electron. Syst.*, pp. 11-20, Jan. 1982.
- [22] P. L. McQuate *et al.*, "Tabulations of propagation data over irregular terrain in the 230-9200 MHz frequency range," U.S. Dep. Commerce, ESSA Rep. ERL-65-ITS-58, Mar. 1968.

Raymond J. Luebbers (S'72-M'76), for a photograph and biography please see page 1098 of the November 1982 issue of this TRANSACTIONS.